Quantum interference of electrons in Ta_4Te_4Si

A. Stolovits* and A. Sherman
Tartu Ülikooli Füüsika Instituut, Riia 142, EE-51014 Tartu, Estonia

K. Ahn and R. K. Kremer
Max-Planck-Institut für Festkörperforschung, Heisenbergstrasse 1, D-70569 Stuttgart, Germany
(Received 17 May 2000; revised manuscript received 11 July 2000)

Transport properties of single crystalline quasi-one-dimensional fibers of Ta_4Te_4Si are studied. The temperature dependence of the resistivity indicates metallic behavior with a residual resistivity ratio of approximately 3. Low-temperature magnetoresistance is positive and anisotropic. The results are interpreted in the framework of the three-dimensional weak localization theory with an anisotropic diffusion constant. Dephasing scattering lengths extracted from the magnetoresistance data are well described by a theory of the electron-electron interaction in disordered metals.

I. INTRODUCTION

Quasi-one-dimensional compounds attract considerable attention due to various electronic instabilities such as charge- and spin-density waves and unusual ''normal'' phase features. For example, a charge-density wave with incommensurate lattice distortions along the chain direction was observed in inorganic compound $NbSe_3$.[1] In the organic conductors $(TMTSF)_2X$, known as Bechgaard salts, states with spin-density wave, metallic conductivity, and superconductivity were observed at different pressure and magnetic field.[2] However, some quasi-one-dimensional compounds appeared to be stable against such symmetry-breaking instabilities. For example $Hg_{3-\delta}AsF_6$, $TaSe_3$, and $Tl_2Mo_6Se_6$ are metallic down to 4 K and even exhibit superconductivity at lower temperatures.[3–5] In this connection a search for other one-dimensional systems, which are resistant to the Peierls transition, is of interest.

A decade ago a new quasi-one-dimensional compound Ta_4Te_4Si was synthesized by Badding and DiSalvo.[6] It is built up from Si centered square antiprismatic Ta_4Te_4 infinite chains weakly bound to each other via the Te–Ta van der Waals interactions. According to band-structure calculations this compound is metallic with two half-filled and a twofold degenerate nearly filled conduction bands.[7] The structure of this compound might be resistant to deformations that lower the density-of-states at the Fermi level. However, early experiments did not confirm this prediction—in Refs. 8 and 9 a characteristic temperature dependence of the resistivity similar to that in $NbSe_3$ was observed that points to an instability also in Ta_4Te_4Si.

In this paper we present a magnetoresistance study of crystalline Ta_4Te_4Si fibers. Both, the temperature dependence of the resistivity and the magnetoresistance demonstrate metallic behavior down to 1.7 K. We found that the temperature dependence of the resistivity, which is typical for the charge-density wave and similar to that measured in Refs. 8 and 9, is observed in Ta_4Te_4Si only after the application of a current pulse. Low-field magnetoresistance is interpreted according to the three-dimensional anisotropic weak-localization theory. Carrier phase scattering lengths extracted from the magnetoresistance data are in good agreement with theoretical predictions of electron-electron interactions in disordered metals.

II. EXPERIMENT

Ta_4Te_4Si single crystals are prepared by chemical vapor transport from stoichiometric ratios of powders of the elements Ta, Te, and Si in evacuated silica vessels with $TeCl_4$ used as a transport agent. Samples were heated and kept at 600 °C for 1 day, then at 1100 °C for 2 days, and after that quenched rapidly to room temperature.[6] As a result fibers, approximately 2 mm long and 2–4 μm thick, were formed. X-ray powder-diffraction patterns were obtained with a STOE powder diffractometer using monochromated Cu $K_{\alpha 1}$ radiation. Crystals invariably exhibited an extreme needlelike shapes with the needle axis colinear with the crystallographic c axis.

For resistivity measurements a fiber was glued with a silver paste to four gold wires separated by 0.5 mm. The resistance was measured by a four-probe technique using a dc nanovoltmeter HP 34420A and the Keithley 2400 current source. The current through the sample was 10 μA, which is low enough to prevent self-heating. We avoided static electricity discharges and current overshoots during contacting the electrical circuit, since they may irreversibly alter the sample properties. Sample mountings were done under dried argon atmosphere because samples are air and moisture sensitive.

Measurements were performed using a variable temperature Oxford ^{4}He cryostat with a superconducting magnet. The rotatable sample holder with an axis perpendicular to the magnetic field allows us to align the fiber either perpendicular or nearly parallel to the magnetic field. Alignment was determined from the extremes of the angular dependence of resistivity. In the case of parallel orientation a small misalignment could arise if the sample and the holder rotation axis were not exactly perpendicular. Magnetoresistance was measured by stabilizing the temperature with an accuracy of ± 0.01 K at a value between 1.5–15 K.

The measurements with the inversion of the magnetic

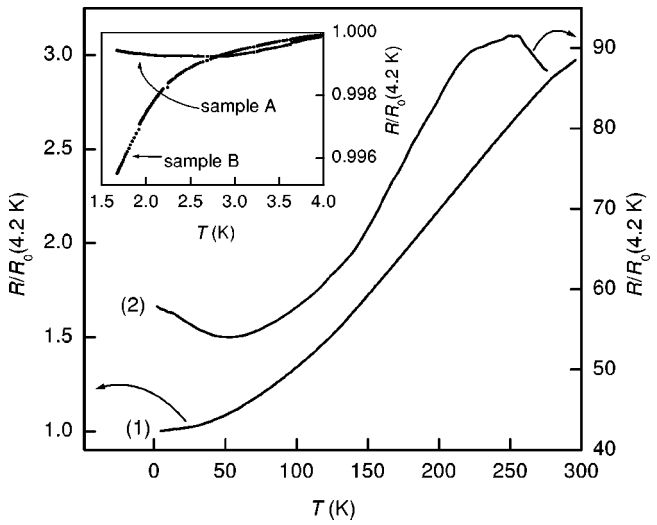

FIG. 1. The temperature dependence of the normalized resistance measured before (1) and after (2) the application of a current pulse (see the text). The curve (2) is normalized to the value of resistance at 4.2 K observed before application of the pulse. Inset: the low-temperature resistance of two different samples from the same batch.

field reveal a weak linear Hall component, which is an indication of nonuniform contacts. In the data analysis this component was subtracted.

III. RESULTS AND DISCUSSION

Figure 1 shows a typical temperature dependence of the resistance in the range 1.7–300 K. Starting from room temperature the resistance gradually decreases with T and saturates below 10 K typical for metallic behavior (curve 1 in Fig. 1). Depending on the sample, the resistivity ρ_0 at 4.2 K lies in the range of 0.92×10^{-4}–6.0×10^{-4} Ω cm. These values are characteristic for semimetals. The sample dependence of ρ_0 supposedly arises from uncertainty of geometrical dimensions, nonuniform current distribution, or sparse package of conducting rods within a fiber. Indeed, the resistivity ratio $\rho(300\ \mathrm{K})/\rho(4.2\ \mathrm{K})$ is the same for all samples. We take the lowest value $\rho_0=0.92\times10^{-4}$ Ω cm as the best estimate for the resistivity.

Close inspection of the low-temperature region reveals a weak temperature dependence of resistivity, which is essentially sample dependent. For samples A and B resistivity increases and decreases, respectively, by 0.5% and 0.02% in the range 1.7–4 K as shown in the inset of Fig. 1. The magnitude of this effect and its low-temperature character allow us to connect it with the quantum interference corrections to the resistivity. These effects are very sensitive to lattice defects that can lead to qualitatively different behavior of different fibers from the same batch.

As noticed previously, Ta_4Te_4Si samples are very sensitive and require even careful electrical handling.[6] For example, application of a short moderately strong current pulse (24 mA for 50 μs) at 4.2 K raises the resistivity irreversibly by more than one order of magnitude. Also the temperature dependence alters qualitatively. The temperature coefficient becomes negative at $T<40$ K and a local maximum appears around 210 K (curve 2 in Fig. 1). This dependence and the

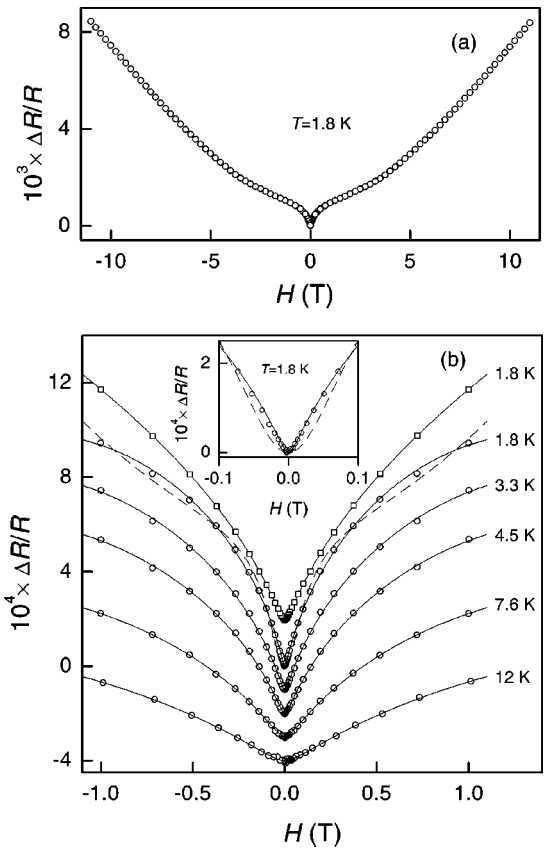

FIG. 2. The normalized magnetoresistance $\Delta R/R=[R(H)-R(0)/R(0)]$ in sample A vs the magnetic field H, aligned along ($\square$) and perpendicular ($\bigcirc$) to the crystallographic c axis. (a) Magnetoresistance in the range of fields up to 11 T. (b) Magnetoresistance in the range of fields up to 1 T for several temperatures. The symbols present experimental data and the solid lines are fits to Eq. (1) for three-dimensional weak-localization corrections. For better visibility curves and symbols are shifted vertically. The dashed line is the best fit of the 1.8 K data to one-dimensional weak-localization corrections. Inset: Magnetoresistance in the range of fields up to 0.1 T with one-dimensional and three-dimensional weak-localization corrections.

value of resistivity are very similar to those measured previously.[8,9] Alterations are attributed to crystal defects induced by the current pulse. We conclude that Ta_4Te_4Si is intrinsically metallic. In the following, we focus on the fibers of Ta_4Te_4Si with a clear metallic temperature character.

Figure 2(a) demonstrates the resistance as a function of the magnetic field H measured in the broad range from -11 T to $+11$ T. The overall magnetoresistance is positive with the classical mechanism dominating in fields above 5 T. The sharp dip in low fields $H<1$ T is a typical fingerprint of the suppression of weak localization by magnetic field.[10] The large-scale electron coherence length L_φ is usually 100–1000 nm and magnetic fields of the order of $\hbar/4eL_\varphi^2$ are necessary for a suppression.[10] The broadening of the magnetoresistance peak with increasing temperature reflects the decrease of L_φ due to both electron-electron and electron-phonon scattering. The magnetoresistance is anisotropic due to the chain structure of the compound. In fields parallel to the chains the magnetoresistance behavior is always broader (L_φ is shorter) than in the perpendicular field orientation.

The anisotropy in the plane perpendicular to the chain is 10% or less.

For a quantitative analysis the dimensionality of weak localization corrections in the quasi-one-dimensional compound is of great importance. One-dimensional behavior is expected either when the fiber cross section is smaller than L_φ or when the electron interchain coupling is so weak that electrons move coherently only within a single chain.[11] Otherwise the system behaves as an anisotropic three-dimensional conductor. Using various models of magnetoresistance we have estimated L_φ to lie in the range 60–300 nm. It is smaller than the thickness of the thinnest fiber and much larger than the interchain separation. Thus, we may assume three-dimensional localization corrections.

We use anisotropic three-dimensional theory of quantum interference corrections to resistivity, which includes weak localization and electron-electron interaction effects.[12,13] In the limit of low fields and strong spin-orbit scattering the relative change of the resistance for the current along the chain axis is expressed by the formula[12–14]

$$\frac{R(H_i)-R(0)}{R(0)}=\alpha_i\rho_0\frac{e^2}{4\pi^2\hbar}\gamma^{3/4}\frac{1}{L_{\varphi\perp}}f_3\left(\frac{4eL_{\varphi i}^2H_i}{\hbar}\right)\times\sqrt{\frac{4eL_{\varphi i}^2H_i}{\hbar}}+BH_i^2, \quad (1)$$

where the index $i=\perp$ or $\parallel$ in H_i, α_i, and $L_{\varphi i}$ corresponds to the direction of the magnetic field perpendicular and parallel to the chain axis, $L_{\varphi i}$ are connected with the phase-braking time τ_φ by the relations $L_{\varphi\parallel}=\sqrt{D_t\tau_\varphi}$ and $L_{\varphi\perp}=(D_tD_l)^{1/4}\sqrt{\tau_\varphi}$ with the diffusion constants D_t and D_l perpendicular and parallel to the chain axis $\gamma=D_l/D_t$, and $f_3\,(1/x)=2\,[\sqrt{2+x}-\sqrt{x}]-[(0.5+x)^{-1/2}+(1.5+x)^{-1/2}]+(2.03+x)^{-3/2}/48$.[15] The first term in the right-hand side of Eq. (1) describes the weak antilocalization correction in the singlet channel of electron diffusion. This term with $\alpha=0.5$ is dominant for heavy element compounds where spin-orbit scattering time τ_{so} is much shorter than τ_φ. The second, quadratic term contains contributions from the classical magnetoresistance mechanism, weak localization in the triplet channel, spin splitting,[16] and electron-electron scattering in the limit of low fields, $H\ll\hbar/4eD\tau_{so}$, $H\ll k_BT/g\mu_B$, and $H\ll\pi k_BT/2eD$, where k_B is the Boltzmann constant, μ_B is the Bohr magneton, and g is the gyromagnetic ratio.

In superconductors, above the critical temperature T_c, scattering on virtual Cooper pairs (the Maki-Thompson-Larkin effect) contributes also to the resistivity and this contribution is described by the first term of Eq. (1) with the temperature-dependent coefficient $\alpha=\beta(T/T_c)$, where β is the function tabulated in Ref. 17.

We fit the magnetoresistance data to Eq. (1) using α_i, $L_{\varphi i}$, and B as fitting parameters. These fits shown as solid lines in Fig. 2(b) are in very good agreement with the experimental data for all temperatures and for both orientations of the magnetic fields. The standard deviation value of 6×10^{-6} is comparable with the measurement accuracy. Other models of the magnetoresistance describe experimental dependencies much worse. For example, the one-dimensional weak localization correction with the quadratic classical magnetoresistance term[18] $[R(H)-R(0)]/R(0)=a_1[1+(H/a_2)^2]^{-1/2}-a_1+a_3H^2$ ($a_1=-7.03\times10^{-4}$, $a_2=85.4$ mT, $a_3=3.21\times10^{-4}T^{-2}$) gives 3.4 times larger standard deviation and does not fit the experimental behavior both in low- and high-field regions [see the dashed curves in Fig. 2(b) and in its inset].

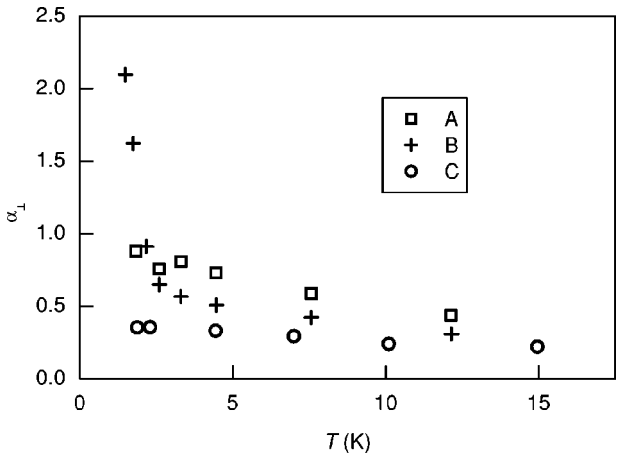

FIG. 3. Temperature dependence of the coefficient α in Eq. (1) for samples A, B, and C, respectively.

The anisotropy of magnetoresistance was measured only at the lowest temperature $T=1.8$ K to diminish the overlap of the quantum-mechanical and classical magnetoresistance components in the case of the parallel field orientation. In sample A we get $L_{\varphi\parallel}=137$ nm, $L_{\varphi\perp}=246$ nm, and $\gamma=10$. The anisotropy of samples B and C is larger—$\gamma=17$ and 29, respectively. In the subsequent analysis these values will be used for temperatures up to 15 K. In this range the resistivity saturates indicating to the constant value of the diffusion constant. α_i depends on the direction of magnetic field and the ratio $\alpha_\parallel/\alpha_\perp$ is 1.8, 2.2, and 1.9 in samples A, B, and C, respectively. Possibly, this anisotropy indicates the nonuniversal behavior of the three-dimensional weak localization.[11]

The temperature dependence of the coefficient $\alpha_\perp$ in Eq. (1) is shown in Fig. 3. Above 10 K it reaches the values 0.24–0.44, close to the theoretical value $\alpha_\perp=0.5$, if we take into account the uncertainty of ρ_0 as previously mentioned. With decreasing temperature, $\alpha_\perp$ increases in all samples. This effect is especially noticeable for sample B in which $\alpha_\perp$ increases steeply at temperatures below 2.5 K. This strong temperature dependence, which correlates with the temperature dependence of the resistance (see inset of Fig. 1) allows us to connect this behavior with the Maki-Thompson-Larkin effect. Strong superconducting fluctuations allow us to expect the superconducting transition in this compound at sub-Kelvin temperatures. Additional experiments are necessary to verify this supposition.

The temperature dependence of $L_{\varphi\perp}$ in samples A, B, and C is shown in Fig. 4. For $T>3$ K the data follow the power law

$$L_{\varphi\perp}^{-2}=KT^{3/2}, \quad (2)$$

with $K=4.17$ $\mu m^{-2}K^{-3/2}$. As known, the same temperature dependence is given by electron-electron scattering with small energy transfer in three-dimensional disordered metals[19]

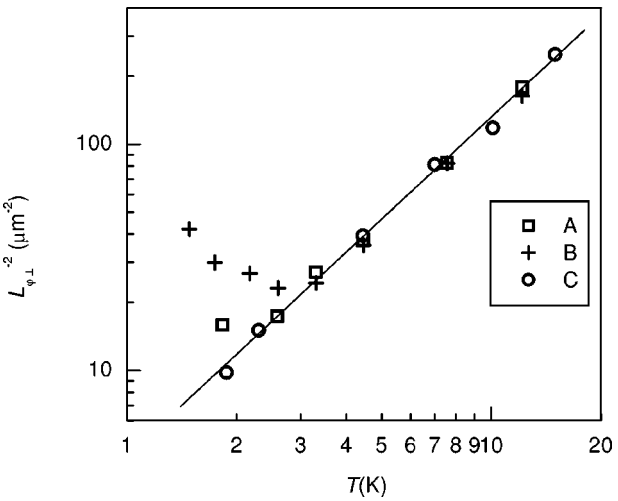

FIG. 4. The inverse square of the dephasing length $L_{\varphi\perp}$ vs temperature. Symbols represent experimental data and the solid line is the best fit with $L_{\varphi\perp}^{-2}=KT^{3/2}$, $K=4.17\ \mu\mathrm{m}^{-2}\,\mathrm{K}^{-3/2}$.

$$\tau_{\mathrm{e\text{-}e}}^{-1}=\frac{(k_BT)^{3/2}}{12\sqrt{2}\pi 3\hbar^{5/2}\nu\tilde{D}^{3/2}}, \tag{3}$$

where ν is the electron density-of-states on the Fermi level and $\tilde{D}=(D_lD_t^2)^{1/3}$. To estimate K we use $\nu=13.3\ \mathrm{eV}^{-1}\,\mathrm{nm}^{-3}$, which was deduced from the band-structure calculations[7] and $D_l=5.1\ \mathrm{cm}^2/\mathrm{s}$ calculated from Einstein's relation $1/\rho_0=e^2\nu D_l$ with the experimentally determined ρ_0. We get $K=0.055$–$0.27\ \mu\mathrm{m}^{-2}\,\mathrm{K}^{-3/2}$, which corresponds to $\gamma=10$ and 29 for the lower and upper limits of this range. The agreement with experiment is acceptable taking into account the strong dependence of K on $D(K\sim D^{-5/2})$.

In sample B, for low temperatures $T<3$ K the dependence $L_{\varphi\perp}^{-2}(T)$ deviates significantly from the $T^{3/2}$ law. The negative temperature coefficient in this temperature range correlates with the peculiarities in temperature behavior of R and $\alpha_\perp$ (see Figs. 1 and 3) and can be associated with the larger contrribution from superconducting fluctuations.[20] The analogous behavior was observed earlier in Al films[21] and Ti-Al-(Sn,Co) alloys.[22]

In conclusion, we studied the magnetoresistance and electron decoherence in metallic Ta_4Te_4Si samples. For T in the range 3–15 K, electron decoherence is satisfactorily described by the theory of electron-electron scattering. The quantum interference contribution to the magnetoresistance is interpreted in the framework of three-dimensional weak localization theory in the limit of strong spin-orbit scattering.

ACKNOWLEDGMENTS

The authors thank J. Engering and E. Peters for the sample characterization with an electron microscope. This work was supported in part by the Estonian Science Foundation Grant No. 3872. A.St. kindly acknowledges support from the Max-Planck-Gesellschaft for a Forschungsstipendium.

*Electronic address: andres@fi.tartu.ee

[1] For a review, see G. Grüner, Rev. Mod. Phys. **60**, 1129 (1988).
[2] T. Ishiguro and K. Yamaji, *Organic Superconductors* (Springer-Verlag, Berlin, 1990).
[3] D.P. Chakraborty, R. Spal, A.M. Denenstein, K.B. Lee, A.J. Heeger, and M.Ya. Azbel, Phys. Rev. Lett. **43**, 1832 (1979).
[4] T. Sambongi, M. Yamamoto, K. Tsutsumi, Y. Shiozaki, K. Yamaya, and Y. Abe, J. Phys. Soc. Jpn. **42**, 1421 (1977).
[5] J.C. Armici, M. Decroux, Ø. Fischer, M. Potel, R. Chevrel, and M. Sergent, Solid State Commun. **33**, 607 (1980).
[6] M.E. Badding and F.J. DiSalvo, Inorg. Chem. **29**, 3952 (1990).
[7] J. Li, R. Hoffmann, M.E. Badding, and F.J. DiSalvo, Inorg. Chem. **29**, 3943 (1990).
[8] M.E. Badding, R.L. Gitzendanner, R.P. Ziebarth, and F.J. DiSalvo, Mater. Res. Bull. **29**, 327 (1994).
[9] K. Ahn, T. Hughbanks, K.D.D. Rathnayaka, and D.G. Naugle, Chem. Mater. **6**, 418 (1994).
[10] B. L. Altshuler and A. G. Aronov, in *Electron-Electron Interactions in Disordered Systems*, edited by M. Pollak and A. M. Efros (North-Holland, Amsterdam, 1985).
[11] C. Mauz, A. Rosch, and P. Wölfle, Phys. Rev. B **56**, 10 953 (1997).
[12] A. Kawabata, J. Phys. Soc. Jpn. **49**, 628 (1980).
[13] B.L. Altshuler, A.G. Aronov, A.I. Larkin, and D.E. Khmelnitskii, Zh. Éksp. Teor. Fiz. **81**, 768 (1981) [Sov. Phys. JETP **54**, 411 (1981)].
[14] W. Szott, C. Jedrzek, and W.P. Kirk, Phys. Rev. B **40**, 1790 (1989).
[15] D.V. Baxter, R. Richter, M.L. Trudeau, R.W. Cochrane, and J.O. Strom-Olsen, J. Phys. (France) **50**, 1673 (1989).
[16] P.A. Lee and T.V. Ramakrishnan, Phys. Rev. B **26**, 4009 (1982).
[17] A.I. Larkin, Pis'ma Zh. Éksp. Teor. Fiz. **31**, 239 (1980) [JETP Lett. **31**, 219 (1980)].
[18] B.L. Altshuler and A.G. Aronov, Pis'ma Zh. Éksp. Teor. Fiz. **33**, 515 (1981) [JETP Lett. **33**, 499 (1981)].
[19] B.L. Altshuler and A.G. Aronov, Pis'ma Zh. Éksp. Teor. Fiz. **30**, 514 (1979) [JETP Lett. **30**, 482 (1979)]; B.L. Altshuler and A.G. Aronov, Solid State Commun. **38**, 11 (1981).
[20] W. Brenig, M. Chang, E. Abrahams, and P. Wölfle, Phys. Rev. B **31**, 7001 (1985).
[21] J.M. Gordon, C.J. Lobb, and M. Tinkham, Phys. Rev. B **29**, 5232 (1984).
[22] C.Y. Wu and J.J. Lin, Phys. Rev. B **50**, 385 (1994).